Belle preprint *2022-03*
KEK preprint *2021-62*

arXiv:2203.05320v1 [hep-ex] 10 Mar 2022

Search for $B^0 \to K^0_S K^0_S \gamma$ decays at Belle

H. B. Jeon,[47,*] K. H. Kang,[42] H. Park,[47] I. Adachi,[21,17] H. Aihara,[90] S. Al Said,[83,43] D. M. Asner,[3] H. Atmacan,[8] T. Aushev,[23] R. Ayad,[83] V. Babu,[9] S. Bahinipati,[27] P. Behera,[30] K. Belous,[34] J. Bennett,[57] F. Bernlochner,[2] M. Bessner,[20] V. Bhardwaj,[26] B. Bhuyan,[28] T. Bilka,[5] A. Bobrov,[4,69] D. Bodrov,[23,48] J. Borah,[28] A. Bozek,[66] M. Bračko,[54,40] P. Branchini,[36] T. E. Browder,[20] A. Budano,[36] M. Campajola,[35,61] D. Červenkov,[5] M.-C. Chang,[13] P. Chang,[65] A. Chen,[63] B. G. Cheon,[19] K. Chilikin,[48] H. E. Cho,[19] K. Cho,[45] S.-J. Cho,[96] S.-K. Choi,[7] Y. Choi,[81] S. Choudhury,[38] D. Cinabro,[94] S. Cunliffe,[9] S. Das,[53] N. Dash,[30] G. De Pietro,[36] R. Dhamija,[29] F. Di Capua,[35,61] J. Dingfelder,[2] Z. Doležal,[5] T. V. Dong,[11] D. Epifanov,[4,69] T. Ferber,[9] D. Ferlewicz,[56] B. G. Fulsom,[72] R. Garg,[73] V. Gaur,[93] N. Gabyshev,[4,69] A. Giri,[29] P. Goldenzweig,[41] B. Golob,[50,40] E. Graziani,[36] T. Gu,[74] K. Gudkova,[4,69] C. Hadjivasiliou,[72] T. Hara,[21,17] K. Hayasaka,[68] H. Hayashii,[62] M. T. Hedges,[20] T. Higuchi,[42] W.-S. Hou,[65] C.-L. Hsu,[82] K. Inami,[60] G. Inguglia,[33] A. Ishikawa,[21,17] R. Itoh,[21,17] M. Iwasaki,[71] Y. Iwasaki,[21] W. W. Jacobs,[31] E.-J. Jang,[18] S. Jia,[14] Y. Jin,[90] K. K. Joo,[6] J. Kahn,[41] H. Kakuno,[92] A. B. Kaliyar,[84] T. Kawasaki,[44] C. Kiesling,[55] C. H. Kim,[19] D. Y. Kim,[80] K.-H. Kim,[96] K. T. Kim,[46] Y.-K. Kim,[96] K. Kinoshita,[8] P. Kodyš,[5] T. Konno,[44] A. Korobov,[4,69] S. Korpar,[54,40] E. Kovalenko,[4,69] P. Križan,[50,40] R. Kroeger,[57] P. Krokovny,[4,69] T. Kuhr,[51] M. Kumar,[53] K. Kumara,[94] A. Kuzmin,[4,69,48] Y.-J. Kwon,[96] Y.-T. Lai,[42] K. Lalwani,[53] T. Lam,[93] J. S. Lange,[15] M. Laurenza,[36,77] S. C. Lee,[47] C. H. Li,[49] J. Li,[47] Y. Li,[14] Y. B. Li,[14] L. Li Gioi,[55] J. Libby,[30] K. Lieret,[51] D. Liventsev,[94,21] A. Martini,[97] M. Masuda,[89,75] T. Matsuda,[58] D. Matvienko,[4,69,48] S. K. Maurya,[28] M. Merola,[35,61] F. Metzner,[41] K. Miyabayashi,[62] R. Mizuk,[48,23] G. B. Mohanty,[84] M. Nakao,[21,17] D. Narwal,[28] Z. Natkaniec,[66] A. Natochii,[20] L. Nayak,[29] M. Nayak,[86] N. K. Nisar,[3] S. Nishida,[21,17] K. Ogawa,[68] S. Ogawa,[87] H. Ono,[67,68] Y. Onuki,[90] P. Oskin,[48] P. Pakhlov,[48,59] G. Pakhlova,[23,48] T. Pang,[74] S. Pardi,[35] S.-H. Park,[21] A. Passeri,[36] S. Patra,[26] S. Paul,[85,55] T. K. Pedlar,[52] R. Pestotnik,[40] L. E. Piilonen,[93] T. Podobnik,[50,40] V. Popov,[23] E. Prencipe,[24] M. T. Prim,[2] M. V. Purohit,[70] M. Röhrken,[9] A. Rostomyan,[9] N. Rout,[30] G. Russo,[61] D. Sahoo,[38] S. Sandilya,[29] A. Sangal,[8] L. Santelj,[50,40] T. Sanuki,[88] V. Savinov,[74] G. Schnell,[1,25] C. Schwanda,[33] Y. Seino,[68] K. Senyo,[95] M. E. Sevior,[56] M. Shapkin,[34] C. Sharma,[53] V. Shebalin,[20] C. P. Shen,[14] J.-G. Shiu,[65] J. B. Singh,[73,†] A. Sokolov,[34] E. Solovieva,[48] M. Starič,[40] Z. S. Stottler,[93] J. F. Strube,[72] M. Sumihama,[16,75] T. Sumiyoshi,[92] M. Takizawa,[79,22,76] U. Tamponi,[37] K. Tanida,[39] F. Tenchini,[9] M. Uchida,[91] T. Uglov,[48,23] Y. Unno,[19] S. Uno,[21,17] P. Urquijo,[56] Y. Usov,[4,69] S. E. Vahsen,[20] R. Van Tonder,[2] G. Varner,[20] K. E. Varvell,[82] A. Vinokurova,[4,69] A. Vossen,[10] E. Waheed,[21] C. H. Wang,[64] M.-Z. Wang,[65] S. Watanuki,[96] E. Won,[46] B. D. Yabsley,[82] W. Yan,[78] S. B. Yang,[46] H. Ye,[9] J. Yelton,[12] J. H. Yin,[46] C. Z. Yuan,[32] Y. Yusa,[68] Y. Zhai,[38] Z. P. Zhang,[78] V. Zhilich,[4,69] and V. Zhukova[48]

(The Belle Collaboration)

[1] *Department of Physics, University of the Basque Country UPV/EHU, 48080 Bilbao*
[2] *University of Bonn, 53115 Bonn*
[3] *Brookhaven National Laboratory, Upton, New York 11973*
[4] *Budker Institute of Nuclear Physics SB RAS, Novosibirsk 630090*
[5] *Faculty of Mathematics and Physics, Charles University, 121 16 Prague*
[6] *Chonnam National University, Gwangju 61186*
[7] *Chung-Ang University, Seoul 06974*
[8] *University of Cincinnati, Cincinnati, Ohio 45221*
[9] *Deutsches Elektronen–Synchrotron, 22607 Hamburg*
[10] *Duke University, Durham, North Carolina 27708*
[11] *Institute of Theoretical and Applied Research (ITAR), Duy Tan University, Hanoi 100000*
[12] *University of Florida, Gainesville, Florida 32611*
[13] *Department of Physics, Fu Jen Catholic University, Taipei 24205*
[14] *Key Laboratory of Nuclear Physics and Ion-beam Application (MOE) and Institute of Modern Physics, Fudan University, Shanghai 200443*
[15] *Justus-Liebig-Universität Gießen, 35392 Gießen*
[16] *Gifu University, Gifu 501-1193*
[17] *SOKENDAI (The Graduate University for Advanced Studies), Hayama 240-0193*
[18] *Gyeongsang National University, Jinju 52828*
[19] *Department of Physics and Institute of Natural Sciences, Hanyang University, Seoul 04763*

[20] *University of Hawaii, Honolulu, Hawaii 96822*
[21] *High Energy Accelerator Research Organization (KEK), Tsukuba 305-0801*
[22] *J-PARC Branch, KEK Theory Center, High Energy Accelerator Research Organization (KEK), Tsukuba 305-0801*
[23] *National Research University Higher School of Economics, Moscow 101000*
[24] *Forschungszentrum Jülich, 52425 Jülich*
[25] *IKERBASQUE, Basque Foundation for Science, 48013 Bilbao*
[26] *Indian Institute of Science Education and Research Mohali, SAS Nagar, 140306*
[27] *Indian Institute of Technology Bhubaneswar, Satya Nagar 751007*
[28] *Indian Institute of Technology Guwahati, Assam 781039*
[29] *Indian Institute of Technology Hyderabad, Telangana 502285*
[30] *Indian Institute of Technology Madras, Chennai 600036*
[31] *Indiana University, Bloomington, Indiana 47408*
[32] *Institute of High Energy Physics, Chinese Academy of Sciences, Beijing 100049*
[33] *Institute of High Energy Physics, Vienna 1050*
[34] *Institute for High Energy Physics, Protvino 142281*
[35] *INFN - Sezione di Napoli, I-80126 Napoli*
[36] *INFN - Sezione di Roma Tre, I-00146 Roma*
[37] *INFN - Sezione di Torino, I-10125 Torino*
[38] *Iowa State University, Ames, Iowa 50011*
[39] *Advanced Science Research Center, Japan Atomic Energy Agency, Naka 319-1195*
[40] *J. Stefan Institute, 1000 Ljubljana*
[41] *Institut für Experimentelle Teilchenphysik, Karlsruher Institut für Technologie, 76131 Karlsruhe*
[42] *Kavli Institute for the Physics and Mathematics of the Universe (WPI), University of Tokyo, Kashiwa 277-8583*
[43] *Department of Physics, Faculty of Science, King Abdulaziz University, Jeddah 21589*
[44] *Kitasato University, Sagamihara 252-0373*
[45] *Korea Institute of Science and Technology Information, Daejeon 34141*
[46] *Korea University, Seoul 02841*
[47] *Kyungpook National University, Daegu 41566*
[48] *P.N. Lebedev Physical Institute of the Russian Academy of Sciences, Moscow 119991*
[49] *Liaoning Normal University, Dalian 116029*
[50] *Faculty of Mathematics and Physics, University of Ljubljana, 1000 Ljubljana*
[51] *Ludwig Maximilians University, 80539 Munich*
[52] *Luther College, Decorah, Iowa 52101*
[53] *Malaviya National Institute of Technology Jaipur, Jaipur 302017*
[54] *Faculty of Chemistry and Chemical Engineering, University of Maribor, 2000 Maribor*
[55] *Max-Planck-Institut für Physik, 80805 München*
[56] *School of Physics, University of Melbourne, Victoria 3010*
[57] *University of Mississippi, University, Mississippi 38677*
[58] *University of Miyazaki, Miyazaki 889-2192*
[59] *Moscow Physical Engineering Institute, Moscow 115409*
[60] *Graduate School of Science, Nagoya University, Nagoya 464-8602*
[61] *Università di Napoli Federico II, I-80126 Napoli*
[62] *Nara Women's University, Nara 630-8506*
[63] *National Central University, Chung-li 32054*
[64] *National United University, Miao Li 36003*
[65] *Department of Physics, National Taiwan University, Taipei 10617*
[66] *H. Niewodniczanski Institute of Nuclear Physics, Krakow 31-342*
[67] *Nippon Dental University, Niigata 951-8580*
[68] *Niigata University, Niigata 950-2181*
[69] *Novosibirsk State University, Novosibirsk 630090*
[70] *Okinawa Institute of Science and Technology, Okinawa 904-0495*
[71] *Osaka City University, Osaka 558-8585*
[72] *Pacific Northwest National Laboratory, Richland, Washington 99352*
[73] *Panjab University, Chandigarh 160014*
[74] *University of Pittsburgh, Pittsburgh, Pennsylvania 15260*
[75] *Research Center for Nuclear Physics, Osaka University, Osaka 567-0047*
[76] *Meson Science Laboratory, Cluster for Pioneering Research, RIKEN, Saitama 351-0198*
[77] *Dipartimento di Matematica e Fisica, Università di Roma Tre, I-00146 Roma*
[78] *Department of Modern Physics and State Key Laboratory of Particle Detection and Electronics, University of Science and Technology of China, Hefei 230026*
[79] *Showa Pharmaceutical University, Tokyo 194-8543*
[80] *Soongsil University, Seoul 06978*
[81] *Sungkyunkwan University, Suwon 16419*
[82] *School of Physics, University of Sydney, New South Wales 2006*

[83] Department of Physics, Faculty of Science, University of Tabuk, Tabuk 71451
[84] Tata Institute of Fundamental Research, Mumbai 400005
[85] Department of Physics, Technische Universität München, 85748 Garching
[86] School of Physics and Astronomy, Tel Aviv University, Tel Aviv 69978
[87] Toho University, Funabashi 274-8510
[88] Department of Physics, Tohoku University, Sendai 980-8578
[89] Earthquake Research Institute, University of Tokyo, Tokyo 113-0032
[90] Department of Physics, University of Tokyo, Tokyo 113-0033
[91] Tokyo Institute of Technology, Tokyo 152-8550
[92] Tokyo Metropolitan University, Tokyo 192-0397
[93] Virginia Polytechnic Institute and State University, Blacksburg, Virginia 24061
[94] Wayne State University, Detroit, Michigan 48202
[95] Yamagata University, Yamagata 990-8560
[96] Yonsei University, Seoul 03722
[97] Deutsches Elektronen-Synchrotron, 22607 Hamburg

We report the first search for the penguin-dominated process $B^0 \to K^0_S K^0_S \gamma$ using the full data sample of 772×10^6 $B\bar{B}$ pairs collected with the Belle detector at the KEKB asymmetric-energy e^+e^- collider. We do not observe any statistically significant signal yield in the K^0_S-pair invariant mass range 1 GeV/c^2 $< M_{K^0_S K^0_S} <$ 3 GeV/c^2, and set the following upper limits at 90% confidence level: $\mathcal{B}(B^0 \to K^0_S K^0_S \gamma) < 5.8 \times 10^{-7}$, $\mathcal{B}(B^0 \to f_2\gamma) \times \mathcal{B}(f_2(1270) \to K^0_S K^0_S) < 3.1 \times 10^{-7}$, and $\mathcal{B}(B^0 \to f'_2\gamma) \times \mathcal{B}(f'_2(1525) \to K^0_S K^0_S) < 2.1 \times 10^{-7}$. Further, 90% confidence upper limits have also been set in the range of [0.7–2.9]$\times 10^{-7}$ on the $B^0 \to K^0_S K^0_S \gamma$ branching fraction in bins of $M_{K^0_S K^0_S}$.

Radiative $b \to s\gamma$ and $b \to d\gamma$ quark transitions are flavor-changing-neutral-current processes and not allowed at the tree level in the Standard Model (SM). Such decays proceed predominantly through the radiative loop diagrams and are sensitive to the contributions from non-SM particles which may enter the loop diagram. For example, the two-Higgs-doublet model (2HDM) introduces an additional Higgs doublet and the charged Higgs may appear in the loop instead of a W boson. Wilson coefficients in the operator product expansion [1] are modified to include the effect of the 2HDM [2] and this new term depends on the mass of the charged Higgs [3]. Thus, any disparity in the branching fraction from the SM expectations can be interpreted as a new physics contribution.

Branching fractions of several exclusive $b \to s\gamma$ modes have been measured: $B \to K^*\gamma$ [4]; $B \to K_1(1270)\gamma$ [5]; $B \to \phi K\gamma$ [6]; $B \to K\eta'\gamma$ [7]; $B \to K\eta\gamma$ [8]. On the other hand, $B \to \rho\gamma$ and $B \to \omega\gamma$ are the only observed exclusive $b \to d\gamma$ modes [9], and a further study of an additional exclusive mode is important to constrain the ratio of Cabibbo-Kobayashi-Maskawa matrix elements $|V_{td}/V_{ts}|$ [10] and also to test the theoretical models.

The $B^0 \to K^0_S K^0_S \gamma$ decay shown in Fig. 1 is one such radiative electroweak penguin process that proceeds via $b \to d\gamma$ at the quark level. The angular momentum of an intermediate state decaying into two identical neutral pseudoscalar particles, K^0_S, is even due to Bose-Einstein statistics. The spin of the $K^0_S K^0_S$ system must be at least two by the conservation of angular momentum in the $B^0 \to K^0_S K^0_S \gamma$ decay, since the photon is a massless vector particle. Therefore, spin-2 is the lowest spin state possible for the $K^0_S K^0_S$ system. In this Letter, we present results from a search for the $B^0 \to K^0_S K^0_S \gamma$ decay.

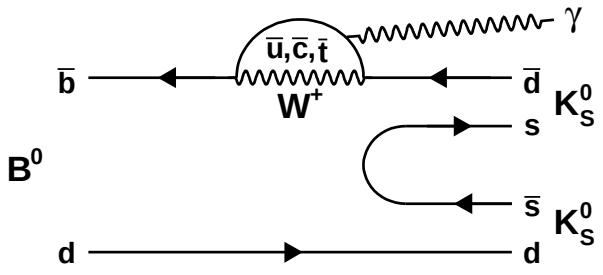


FIG. 1. $b \to d\gamma$ penguin diagram for $B^0 \to K^0_S K^0_S \gamma$ decay.

The $\Upsilon(4S)$ meson is produced at the KEKB asymmetric-energy e^+e^- collider [11] with electrons and positrons having the energes of 8 GeV and 3.5 GeV, respectively, and subsequently decays to $B\bar{B}$ pairs which are nearly at rest in the center-of-mass system (CMS). The z axis is defined opposite to the e^+ beam direction. We search for the decay $B^0 \to K^0_S K^0_S \gamma$ using the full data sample of $(772 \pm 11) \times 10^6$ $B\bar{B}$ pairs collected at the $\Upsilon(4S)$ resonance with the Belle detector at the KEKB asymmetric-energy e^+e^- collider. This is the first ever search for a B^0 decay to two pseudoscalars K^0_S with a prompt photon in the final state. The inclusion of the charge conjugate modes is implied throughout this paper unless otherwise stated.

The Belle detector is a hermetic magnetic spectrome-

* Now at the Enrico Fermi Institute of the University of Chicago, Chicago, IL 60637
† also at University of Petroleum and Energy Studies, Dehradun 248007

ter to detect the decay products of B mesons that consists of a silicon vertex detector, a 50-layer central drift chamber (CDC), an array of aerogel threshold Cherenkov counters, a barrel-like arrangement of time-of-flight scintillation counters, and an electromagnetic calorimeter comprised of CsI(Tl) scintillation crystals (ECL). These detector components, providing high vertex resolution, good tracking, sophisticated particle identification capability, and excellent calorimetry, are located inside a superconducting solenoid coil providing a 1.5 T magnetic field. An iron flux-return is located outside of the magnetic coil which is instrumented to detect K_L^0 mesons and identify muons. The detector is described in detail elsewhere [12].

The event selections are optimized using simulated Monte Carlo (MC) samples. The MC samples for the signal and the backgrounds are generated with EvtGen [13] and the detector response is then simulated using Geant3 [14]. Any environmental changes in the Belle detector and KEKB accelerator machine during the operations are reflected in the detector simulation. To generate the signal MC sample of B^0 decaying to a tensor meson (as an intermediate state) and a prompt photon, a two-body decay model is used with appropriate helicity amplitudes. Then, the intermediate state decays to two K_S^0. As the $K_S^0K_S^0$ structure in $B^0 \to K_S^0K_S^0\gamma$ is unknown, the mass of the intermediate state is evenly distributed between 1 GeV/c^2 and 3 GeV/c^2 in the signal MC sample.

Photons must have no associated tracks in the CDC, be in the ECL barrel region ($33^\circ < \theta_\gamma < 128^\circ$), and have a ratio of energy deposition in 3×3 ECL crystals to that in 5×5 ECL crystals centered on the crystal having the maximum energy above 95%. The CM energy of the prompt photon candidate, E_γ, must satisfy the requirement 1.6 GeV $< E_\gamma <$ 2.8 GeV. Most background photons originate from π^0 and η to $\gamma\gamma$ decays. We combine the photon candidate with all other photons with momenta larger than 50 MeV/c in the event and calculate the probabilities of the reconstructed particle to be π^0-like or η-like [15]. The background photons are suppressed by removing π^0-like and η-like photons by applying selection criteria on a likelihood based selector. About 86% of the photons from the signal B are retained and about 62% from the accompanying B are rejected. For more than one photon satisfying the selection criteria for the prompt photon candidate, the most energetic photon is chosen as the prompt photon candidate. The selection efficiency of the prompt photon is approximately 50% and 99.5% are truly matched photons for the signal MC.

K_S^0 candidates are reconstructed from two oppositely charged tracks. A displaced vertex consistent with $K_S^0 \to \pi^+\pi^-$ decay is required using a neural network (NN) discriminator with 20 inputs [16]; this selection also suppresses $\Lambda \to p\pi^-$ decays. The invariant mass of the pion pairs is then required to satisfy $|M_{\pi\pi} - m_{K_S^0}| < 4.7$ MeV/c^2, corresponding to a $\pm 2.6\sigma$ interval in mass resolution, where $m_{K_S^0}$ is the nominal K_S^0 mass [17]. B^0 candidates are formed by combining two K_S^0 candidates and one prompt photon candidate. The energy difference $\Delta E \equiv E_B^{\rm cms} - E_{\rm beam}^{\rm cms}$ and the beam-energy-constrained mass $M_{\rm bc} \equiv \sqrt{(E_{\rm beam}^{\rm cms})^2 - |\vec{p}_B^{\,\rm cms}|^2c^2}/c^2$, where $E_{\rm beam}^{\rm cms}$ is the beam energy, and $E_B^{\rm cms}$ and $\vec{p}_B^{\,\rm cms}$ are the energy and momentum of the reconstructed B^0, respectively, are used to identify B^0 candidates. The candidates satisfying the requirements 5.20 GeV/$c^2 < M_{\rm bc} <$ 5.29 GeV/c^2 and $|\Delta E| <$ 0.5 GeV are retained for further analysis. We find that 6% of the events have more than one B^0 candidate. In case of multiple candidates, we choose the one with the smallest χ^2 as defined by $\chi^2 = \sum_{i=1}^{2}[(m_{K_S^0} - M_i(\pi^+\pi^-))/\sigma_{\pi\pi}]^2$, where $\sigma_{\pi\pi}$ is the mass resolution for the reconstructed K_S^0.

The dominant background is $e^+e^- \to q\bar{q}$ ($q = u, d, s, c$) continuum events. We use another NN with four input variables calculated in the CMS to suppress this background [18]: the cosine of the polar angle ($\cos\theta_B$) of the B^0 candidate flight direction; the cosine of the angle ($\cos\theta_T$) between the thrust axis of the B^0 candidate and that of the rest of the event; a flavor-tagging quality parameter of the accompanying B meson [19]; and a likelihood ratio obtained from the modified Fox-Wolfram moments [20]. The NN outputs for the signal and continuum MC events peak at +1 and –1, respectively. The figure-of-merit (FOM) is calculated as [21]:

$$\mathrm{FOM} = \frac{\epsilon_S(t)}{a/2 + \sqrt{N_{\rm bkg}(t)}}, \qquad (1)$$

where t is the NN output; $\epsilon_S(t)$ is the signal efficiency as a function of t determined by using the signal MC sample; $N_{\rm bkg}$ is the remaining background events after NN selection and a is taken to be 3 for a 3σ significance due to the low signal-to-background ratio, as suggested in Ref. [21]. The maximal FOM is obtained at 0.93 which rejects 99% of the continuum MC events and retains 37% of the signal MC events. Since we expect a few signal events and relatively large backgrounds, we further suppress the continuum background by using the helicity angle, θ_H, which is the angle between the direction opposite to the B^0 candidate and that of the K_S^0 momentum in the rest frame of the $K_S^0K_S^0$ system. To maximize the FOM, we require $0.24 < |\cos\theta_H| < 0.86$ which removes 60% of the background while retaining 86% of the signal.

We use a Crystal Ball line shape [22] and a first-order polynomial for the signal and mis-reconstructed components, respectively. The signal region is defined as -0.16 GeV $< \Delta E <$ 0.09 GeV and 5.272 GeV/$c^2 < M_{\rm bc} <$ 5.290 GeV/c^2, corresponding to $\pm 3\sigma$ windows. About 99% of B^0 candidates in the signal region correctly match signal B^0 and all of them have the correct

prompt photon as the daugther particle of the signal B^0.

From continuum MC, we estimate 2.2 events in the signal region. In addition to the continuum, various $B\bar{B}$ background sources are also studied. Both neutral and charged $B\bar{B}$ MC samples corresponding to an integrated luminosity six times larger than that of the full data sample are used. We expect 0.3 events from generic $B\bar{B}$ decays in the signal region. The decay $B^0 \to D^0(\to K^0_S\pi^0)K^0$, with a branching fraction of 5.2×10^{-5} [17], is treated separately from the generic $B\bar{B}$ because its ΔE and $M_{\rm bc}$ distributions are different from those of generic $B\bar{B}$ events. We estimate the background contribution from this decay to be 0.1.

A dedicated MC sample comprising of rare B decays is prepared: various decays with branching fractions smaller than $\mathcal{O}(10^{-4})$ are included and their total branching fraction is $\mathcal{O}(10^{-3})$. Rare B decays having one or two K^0_S with γ in the final state can peak in the $M_{\rm bc}$ distribution. The backgrounds from the charged B meson pairs do not show any peak in the ΔE–$M_{\rm bc}$ signal region. On the other hand, the background from the neutral B meson pairs peaks in the signal region and the largest contribution (34%) to the peak comes from $B^0 \to X_{d\bar{d}}(\to K^0_S K^0_S)\gamma$. Herein, $X_{d\bar{d}}$ is a meson composed of a d–$\bar{d}$ quark pair. We regard this as signal because the quark level transition and the final state are the same as for the signal. When we treat this decay mode as a signal by using MC information, the peaking background is removed. Neutral and charged rare B backgrounds are estimated to be 1.0 and 0.9 events in the signal region, respectively.

Four more rare decay modes which are not included in the rare B MC samples are considered: $\mathcal{B}(B^0 \to K^0_S K^0_S \pi^0) < 9 \times 10^{-7}$ [23]; $\mathcal{B}(B^0 \to K^0_S K^0_S \eta) < 1.0 \times 10^{-6}$; $\mathcal{B}(B^0 \to K^0_S \pi^+\pi^-\gamma) = 1.99 \times 10^{-5}$ [24]; $\mathcal{B}(B^0 \to \pi^+\pi^-\pi^+\pi^-\pi^0) < 9.1 \times 10^{-3}$ [17]. The first two decay modes occur via a $b \to s$ quark transition and become background when π^0 or η are replaced by a photon. $B^0 \to K^0_S\pi^+\pi^-\gamma$ decays occur through a $b \to s\gamma$ quark transition and can be mis-identified as the signal. $B^0 \to \pi^+\pi^-\pi^+\pi^-\pi^0$ occurs in the tree level with $b \to u$ and can be mis-identified as the signal when π^0 is replaced by a photon. We estimate that the background contribution from these four decay modes is negligible.

We estimate the total number of background events in the signal region to be 4.5±0.7 via the counting method. To estimate the background events in the signal region using an extended unbinned maximum-likelihood fitting method, we fit the $M_{\rm bc}$ distribution satisfying -0.16 GeV $< \Delta E < 0.09$ GeV with an ARGUS function [25] and a Crystal Ball line shape for the continuum and peaking background, respectively. The fitting parameters of the Crystal Ball line shape are fixed to those for the signal MC. We obtain 5.6±0.8 background events in the signal region. This result is consistent with that of the counting method.

The signal efficiency depends on the reconstructed K^0_S-pair mass ($M_{K^0_S K^0_S}$) as shown in Table I and is obtained by performing an extended unbinned maximum-likelihood fit to the $M_{\rm bc}$ distribution satisfying -0.16 GeV $< \Delta E < 0.09$ GeV and 5.2 GeV/c^2 $< M_{\rm bc} <$ 5.9 GeV/c^2 in ten $M_{K^0_S K^0_S}$ bins of equal sizes between 1 GeV/c^2 and 3 GeV/c^2.

The systematic uncertainties from the number of produced $B\bar{B}$ pairs and the $\Upsilon(4S) \to B^0\bar{B}^0$ branching fraction are 1.4% and 1.2% [17], respectively. The systematic uncertainty in the photon detection efficiency is studied using radiative Bhabha events and estimated to be 2.0% [26]. Using a systematic uncertainty of 0.2% for K^0_S reconstruction efficiency and per track uncertainty in efficiency of 0.4% [27] leads to our estimate of 1.4% for the reconstruction efficiency of two K^0_S. The systematic uncertainty due to the background suppression using the NN selection and π^0/η veto is 0.6% [26]. The signal efficiency depends on $M_{K^0_S K^0_S}$ and the MC statistical uncertainty in the efficiency varies between 0.5% and 0.7% depending on $M_{K^0_S K^0_S}$. The total systematic uncertainty is approximately 3.2% depending on $M_{K^0_S K^0_S}$, and is summarized in Table II.

A total of 9 events are observed in the signal region. As shown in Fig. 2, we obtain 3.8±3.0 signal and 5.6±0.8 background events in the signal region with an extended unbinned maximum-likelihood fit to the $M_{\rm bc}$ distribution with a Crystal Ball line shape including contributions from the peaking background for the signal and an ARGUS function for the background, respectively. The fitting parameters for the signal are fixed to those for the signal MC. The number of the background events in the signal region agrees well with that of the estimated background events in the signal region from MC samples.

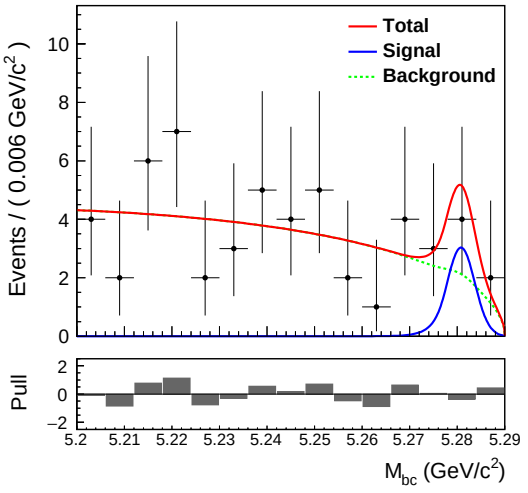


FIG. 2. $M_{\rm bc}$ fit distribution with the signal and background parameterized by a Crystal Ball line shape and an ARGUS function, respectively.

TABLE I. Summary of the number of observed events ($N_{\rm obs}$), number of estimated background events ($N_{\rm bkg}$), efficiencies (ϵ_S), upper limits on the signal yield (S_{90}), and branching fraction upper limits (U.L.) at the 90% C.L. in each $M_{K^0_SK^0_S}$ bin for the $B^0 \to K^0_SK^0_S\gamma$ decay.

mass bin(GeV/c^2)	ϵ_S(%)	$N_{\rm bkg}$	$\sigma_{\rm sys}$(%)	$N_{\rm obs}$	S_{90}	U.L.(10^{-7})
1.0–1.2	3.3	0.8±0.3	3.2	0	1.8	0.7
1.2–1.4	3.0	0.9±0.3	3.2	3	6.5	2.8
1.4–1.6	2.7	0.8±0.3	3.2	1	3.6	1.7
1.6–1.8	2.5	0.3±0.1	3.2	0	2.1	1.1
1.8–2.0	2.3	0.8±0.3	3.2	2	5.1	2.9
2.0–2.2	2.2	0.2±0.1	3.2	1	4.2	2.5
2.2–2.4	2.2	0.4±0.2	3.2	1	3.9	2.4
2.4–2.6	2.2	0.2±0.2	3.2	0	2.2	1.3
2.6–2.8	2.3	0.0±0.0	3.2	1	4.2	2.3
2.8–3.0	2.4	0.1±0.3	3.2	0	2.3	1.2

TABLE II. Systematic uncertainties.

Source	Uncertainty (%)
Number of $B\bar{B}$	1.4
Branching fraction of $\Upsilon(4S) \to B^0\bar{B}^0$	1.2
Photon detection efficiency	2.0
Two K^0_S reconstruction	1.4
NB and π^0/η veto	0.6
MC statistics in $M_{K^0_SK^0_S}$ bin efficiency	0.5–0.7
Total	3.2

The $|\cos\theta_H|$ distributions for events in the $\Delta E - M_{\rm bc}$ signal region are shown in Fig. 3 for data and MC samples. The signal and background MC samples are normalized to have the same yields as obtained by fitting the data in the signal region. The results from data are consistent with MC simulation.

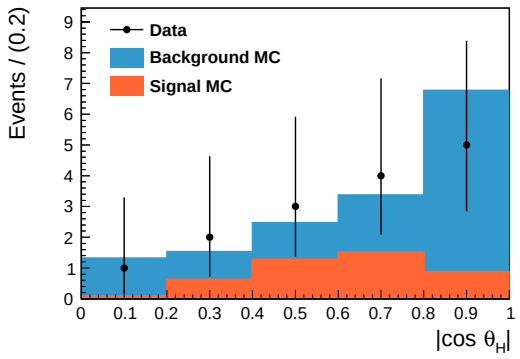


FIG. 3. The helicity angle distribution of the observed events in the signal region.

The observed number of events in each $M_{K^0_SK^0_S}$ bin is obtained by counting the events in the $\Delta E - M_{\rm bc}$ signal region. Figure 4 shows the observed number of events ($N_{\rm obs}$) in the full data sample and the estimated background events in each $M_{K^0_SK^0_S}$ bin. No significant excess over the estimated background is found in data and we derive an upper limit for the signal yield (S_{90}) at the 90% confidence level (C.L.) using the POLE program by taking into account the uncertainties associated with the signal selection efficiency, background expectation, and systematic uncertainty [28]. The branching fractions are obtained from

$$\mathcal{B}(B^0 \to K^0_SK^0_S\gamma) = \frac{S_{90}}{\epsilon_S \times N_{B\bar{B}}}, \qquad (2)$$

where $N_{B\bar{B}}$ and ϵ_S are the number of $B\bar{B}$ pairs and signal efficiency, respectively. We set 90% C.L. upper limits on the partial branching fractions for the decay $B^0 \to K^0_SK^0_S\gamma$ in ten bins of the K^0_S-pair for 1.0 GeV/c^2 < $M_{K^0_SK^0_S}$ < 3.0 GeV/c^2, which are listed in Table I.

For the full range 1.0 GeV/c^2 < $M_{K^0_SK^0_S}$ < 3.0 GeV/c^2, we use the average efficiency of all bins, (2.5±0.4)%. The standard deviation of efficiencies among $M_{K^0_SK^0_S}$ bins is assigned as a systematic uncertainty (16.0%). Adding to other systematic uncertainties listed in Table II in quadrature, the total systematic uncertainty is 16.2%. Using the POLE program with 9 observed events and expected background of 4.5 ± 0.7, we set the upper limit on the branching fraction for the 1.0 GeV/c^2 < $M_{K^0_SK^0_S}$ < 3.0 GeV/c^2 mass range to be 5.8×10^{-7} at the 90% C.L.

We also set upper limits on branching fraction products for intermediate tensor f_2 states, $\mathcal{B}(B^0 \to f_2\gamma) \times \mathcal{B}(f_2 \to K^0_SK^0_S)$. The signal mass regions are taken to be 1.00 GeV/c^2 < $M_{K^0_SK^0_S}$ < 1.44 GeV/c^2 and 1.44 GeV/c^2 < $M_{K^0_SK^0_S}$ < 1.63 GeV/c^2 for $f_2(1270)$ and $f_2'(1525)$, respectively. These mass regions contain 80% of signal events. The results are summarized in Table III.

In summary, we report on the search for radiative B decays with the $K^0_SK^0_S\gamma$ final state using a data sample

TABLE III. Summary of the number of observed events ($N_{\rm obs}$), number of estimated background events ($N_{\rm bkg}$), efficiencies (ϵ_S), upper limits on the signal yield (S_{90}), and branching fraction upper limits (U.L.) at the 90% C.L. for the $B^0 \to f_2\gamma$ and $f_2 \to K^0_S K^0_S$ decays.

Mode	$\epsilon_S(\%)$	$N_{\rm bkg}$	$\sigma_{\rm sys}(\%)$	$N_{\rm obs}$	S_{90}	U.L.(10^{-7})
$B^0 \to f_2(1270)(\to K^0_S K^0_S)\gamma$	2.3	1.8±0.4	3.1	3	5.7	3.1
$B^0 \to f'_2(1525)(\to K^0_S K^0_S)\gamma$	2.2	0.8±0.3	3.1	1	3.6	2.1

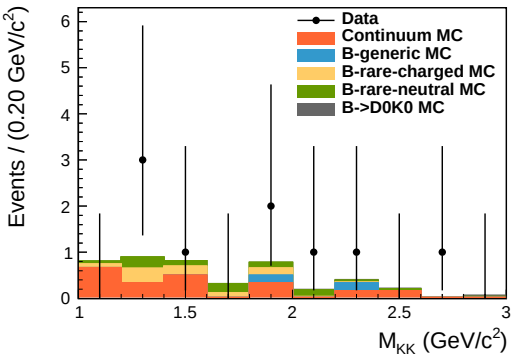


FIG. 4. The $M_{K^0_S K^0_S}$ distribution in the signal region. The dots represent data and the histograms are the estimated number of backgrounds from the MC background samples.

of 772×10^6 $B\bar{B}$ pairs. No significant signal is observed for the full data sample. The signal efficiency depends on $M_{K^0_S K^0_S}$ and we set upper limits at the 90% C.L. on the partial branching fractions for the decay $B^0 \to K^0_S K^0_S \gamma$ in ten bins of the K^0_S-pair for 1.0 GeV/c^2 < $M_{K^0_S K^0_S}$ < 3.0 GeV/c^2 to be [0.7–2.9]$\times 10^{-7}$. We also set an upper limit on its branching fraction as 5.8×10^{-7} at the 90% C.L. for the 1.0 GeV/c^2 < $M_{K^0_S K^0_S}$ < 3.0 GeV/c^2 mass range. The upper limits at the 90% C.L. on the products of the branching fractions $\mathcal{B}(B^0 \to f_2\gamma) \times \mathcal{B}(f_2(1270) \to K^0_S K^0_S)$ and $\mathcal{B}(B^0 \to f'_2\gamma) \times \mathcal{B}(f'_2(1525) \to K^0_S K^0_S)$ are obtained to be 3.1×10^{-7} and 2.1×10^{-7}, respectively. These results for the decay $B^0 \to K^0_S K^0_S \gamma$ are presented for the first time.

We thank the KEKB group for the excellent operation of the accelerator; the KEK cryogenics group for the efficient operation of the solenoid; and the KEK computer group, and the Pacific Northwest National Laboratory (PNNL) Environmental Molecular Sciences Laboratory (EMSL) computing group for strong computing support; and the National Institute of Informatics, and Science Information NETwork 5 (SINET5) for valuable network support. We acknowledge support from the Ministry of Education, Culture, Sports, Science, and Technology (MEXT) of Japan, the Japan Society for the Promotion of Science (JSPS), and the Tau-Lepton Physics Research Center of Nagoya University; the Australian Research Council including grants DP180102629, DP170102389, DP170102204, DP150103061, FT130100303; Austrian Federal Ministry of Education, Science and Research (FWF) and FWF Austrian Science Fund No. P 31361-N36; the National Natural Science Foundation of China under Contracts No. 11435013, No. 11475187, No. 11521505, No. 11575017, No. 11675166, No. 11705209; Key Research Program of Frontier Sciences, Chinese Academy of Sciences (CAS), Grant No. QYZDJ-SSW-SLH011; the CAS Center for Excellence in Particle Physics (CCEPP); the Shanghai Science and Technology Committee (STCSM) under Grant No. 19ZR1403000; the Ministry of Education, Youth and Sports of the Czech Republic under Contract No. LTT17020; Horizon 2020 ERC Advanced Grant No. 884719 and ERC Starting Grant No. 947006 "InterLeptons" (European Union); the Carl Zeiss Foundation, the Deutsche Forschungsgemeinschaft, the Excellence Cluster Universe, and the VolkswagenStiftung; the Department of Atomic Energy (Project Identification No. RTI 4002) and the Department of Science and Technology of India; the Istituto Nazionale di Fisica Nucleare of Italy; National Research Foundation (NRF) of Korea Grant Nos. 2016R1D1A1B-01010135, 2016R1D1A1B02012900, 2018R1A2B3003643, 2018R1A6A1A06024970, 2019K1A3A7A09033840, 2019K1A3A7A09034974, 2019R1I1A3A01058933, 2021R1A6A1A03043957, 2021R1F1A1060423, 2021R1-F1A1064008; Radiation Science Research Institute, Foreign Large-size Research Facility Application Supporting project, the Global Science Experimental Data Hub Center of the Korea Institute of Science and Technology Information and KREONET/GLORIAD; the Polish Ministry of Science and Higher Education and the National Science Center; the Ministry of Science and Higher Education of the Russian Federation, Agreement 14.W03.31.0026, and the HSE University Basic Research Program, Moscow; University of Tabuk research grants S-1440-0321, S-0256-1438, and S-0280-1439 (Saudi Arabia); the Slovenian Research Agency Grant Nos. J1-9124 and P1-0135; Ikerbasque, Basque Foundation for Science, Spain; the Swiss National Science Foundation; the Ministry of Education and the Ministry of Science and Technology of Taiwan; and the United States Department of Energy and the National Science Foundation.

[1] A. J. Buras, Lect. Notes Phys. **558**, 65 (2000).

[2] T. Hurth, E. Lunghi, and W. Porod, Nucl. Phys. B **704**, 56 (2005).

[3] G. C. Branco *et al*., Phys. Rept. **516**, 1 (2012).

[4] R. Aaij *et al*. (LHCb Collaboration), Nucl. Phys. B **867**, 1 (2013); B. Aubert *et al*. (*BABAR* Collaboration), Phys. Rev. Lett. **103**, 211802 (2009); M. Nakao *et al*. (Belle Collaboration), Phys. Rev. D **69**, 112001 (2004); T. E. Coan *et al*. (CLEO Collaboration), Phys. Rev. Lett. **84**, 5283 (2000).

[5] H. Yang *et al*. (Belle Collaboration), Phys. Rev. Lett. **94**, 111802 (2005).

[6] H. Sahoo *et al*. (Belle Collaboration), Phys. Rev. D **84**, 071101(R) (2011); B. Aubert *et al*. (*BABAR* Collaboration), Phys. Rev. D **75**, 051102 (2007); A. Drutskoy *et al*. (Belle Collaboration), Phys. Rev. Lett. **92**, 051801 (2004).

[7] R. Wedd *et al*. (Belle Collaboration), Phys. Rev. D **81**, 111104(R) (2010).

[8] S. Nishida *et al*. (Belle Collaboration), Phys. Lett. B **610**, 23 (2005);

[9] N. Taniguchi *et al*. (Belle Collaboration), Phys. Rev. Lett. **101**, 111801 (2008); B. Aubert *et al*. (*BABAR* Collaboration), Phys. Rev. Lett. **98**, 151802 (2007); D. Mohapatra *et al*. (Belle Collaboration), Phys. Rev. Lett. **96**, 221601 (2006).

[10] M. Kobayashi and T. Maskawa, Prog. Theor. Phys. **49**, 652 (1973); N. Cabibbo, Phys. Rev. Lett. **10**, 531 (1963).

[11] S. Kurokawa and E. Kikutani, Nucl. Instrum. Methods Phys. Res., Sect. A **499**, 1 (2003), and other papers included in this volume; T. Abe *et al*., Prog. Theor. Exp. Phys. **483**, 03A001 (2013), and following articles up to 03A011.

[12] A. Abashian *et al*. (Belle Collaboration), Nucl. Instrum. Methods Phys. Res., Sect. A **479**, 117 (2002); Also, see the detector section in J. Brodzicka *et al*., Prog. Theor. Exp. Phys. **2012**, 04D001 (2012).

[13] D. J. Lange *et al*., Nucl. Instrum. Methods Phys. Res., Sect. A **462**, 152 (2001).

[14] R. Brun *et al*., CERN Report No. CERN DD/EE/84-1, 1984.

[15] P. Koppenburg *et al*. (Belle Collaboration), Phys. Rev. Lett. **93**, 061803 (2004).

[16] H. Nakano, Ph.D. thesis, Tohoku University (2014); H. Nakano *et al*. (Belle Collaboration), Phys. Rev. D **97**, 092003 (2018).

[17] P. A. Zyla *et al*. (Particle Data Group), Prog. Theor. Exp. Phys. **8**, 083C01 (2020).

[18] M. Feindt and U. Kerzel, Nucl. Instrum. Methods Phys. Res., Sect. A **559**, 190 (2006).

[19] H. Kakuno *et al*. (Belle Collaboration), Nucl. Instrum. Methods Phys. Res., Sect. A **533**, 516 (2004).

[20] R. O. Duda, P. E. Hart, and D. G. Stork, Pattern Classification (John Wiley & Sons, New York, 2001), 2nd ed.; G. C. Fox and S. Wolfram, Phys. Rev. Lett. **41**, 1581 (1978); S. H. Lee *et al*. (Belle Collaboration), Phys. Rev. Lett. **91**, 261801 (2003).

[21] G. Punzi, Proceedings of the Statistical problems in particle physics, astrophysics and cosmology, Conference, PHYSTAT 2003, Stanford, USA, eConf C030908, MODT002 (2003).

[22] T. Skwarnicki, Ph.D. thesis, Institute for Nuclear Physics, Krakow (DESY Internal Report No. DESY F31-86-02, 1986).

[23] B. Aubert *et al*. (BABAR Collaboration), Phys. Rev. D **80**, 011101(R) (2009).

[24] H. Yang *et al*. (Belle Collaboration), Phys. Rev. Lett. **94**, 111802 (2005); P. del Amo Sanchez *et al*. (BABAR Collaboration), Phys. Rev. D **93**, 052013 (2016).

[25] H. Albrecht *et al*. (ARGUS Collaboration), Phys. Lett. B **229**, 304 (1989).

[26] T. Horiguchi *et al*. (Belle Collaboration), Phys. Rev. Lett. **119**, 191802 (2017).

[27] S. Jia *et al*. (Belle Collaboration), Phys. Rev. D **100**, 032006 (2019).

[28] J. Conrad *et al*., Phys. Rev. D **67**, 012002 (2003); G. J. Feldman and R. D. Cousins, Phys. Rev. D **57**, 3873 (1998).